

Performance analysis of a solar window incorporating a novel rotationally asymmetrical concentrator

Abu-Bakar, Siti Hawa Binti ; Muhammad-Sukki, Firdaus; Freier, Daria; Ramirez-Iniguez, Roberto; Mallick, Tapas Kumar; Munir, Abu Bakar; Mohd Yasin, Siti Hajar; Mas Ud, Abdullahi Abubakar; Bani, Nurul Aini

Published in:
Energy

DOI:
[10.1016/j.energy.2016.01.006](https://doi.org/10.1016/j.energy.2016.01.006)

Publication date:
2016

Document Version
Author accepted manuscript

[Link to publication in ResearchOnline](#)

Citation for published version (Harvard):

Abu-Bakar, SHB, Muhammad-Sukki, F, Freier, D, Ramirez-Iniguez, R, Mallick, TK, Munir, AB, Mohd Yasin, SH, Mas Ud, AA & Bani, NA 2016, 'Performance analysis of a solar window incorporating a novel rotationally asymmetrical concentrator', *Energy*, vol. 99, pp. 181-192. <https://doi.org/10.1016/j.energy.2016.01.006>

General rights

Copyright and moral rights for the publications made accessible in the public portal are retained by the authors and/or other copyright owners and it is a condition of accessing publications that users recognise and abide by the legal requirements associated with these rights.

Take down policy

If you believe that this document breaches copyright please view our takedown policy at <https://edshare.gcu.ac.uk/id/eprint/5179> for details of how to contact us.

Performance analysis of a solar window incorporating a novel rotationally asymmetrical concentrator

Siti Hawa Abu-Bakar^{a,b,*}, Firdaus Muhammad-Sukki^{c,d}, Daria Freier^a, Roberto Ramirez-Iniguez^a,
Tapas Kumar Mallick^e, Abu Bakar Munir^{f,g}, Siti Hajar Mohd Yasin^h,
Abdullahi Abubakar Mas'udⁱ, Nurul Aini Bani^j

^a School of Engineering & Built Environment, Glasgow Caledonian University, 70 Cowcaddens Road, Glasgow, G4 0BA Scotland, United Kingdom

^b Universiti Kuala Lumpur British Malaysian Institute, Batu 8, Jalan Sungai Pusu, 53100 Gombak, Selangor, Malaysia

^c School of Engineering, Faculty of Design and Technology, Robert Gordon University, Garthdee House, Garthdee Road, Aberdeen, AB10 7QB, Scotland, United Kingdom

^d Faculty of Engineering, Multimedia University, Persiaran Multimedia, 63100 Cyberjaya, Selangor, Malaysia

^e Environment and Sustainability Institute, University of Exeter, Penryn, Cornwall, TR10 9EZ, United Kingdom

^f Faculty of Law, University of Malaya, 50603 Kuala Lumpur, Malaysia

^g University of Malaya Malaysian Centre of Regulatory Studies (UMCoRS), University of Malaya, 59990 Jalan Pantai Baru, Kuala Lumpur, Malaysia

^h Faculty of Law, Universiti Teknologi MARA, 40450 Shah Alam, Malaysia

ⁱ Department of Electrical and Electronic Engineering Technology, Jubail Industrial College, P O Box 10099, Saudi Arabia

^j UTM Razak School of Engineering and Advanced Technology, Universiti Teknologi Malaysia, 54100 Kuala Lumpur, Malaysia

* Phone/Fax number: +44(0)141 273 1482/+44(0)141 331 3690, e-mail: sitihawa.abubakar@gcu.ac.uk / hawa012@gmail.com

Abstract: The race towards achieving a sustainable zero carbon building has spurred the introduction of many new technologies, including the building integrated photovoltaic (BIPV) system. To tackle the high capital cost of BIPV systems, low-concentration photovoltaic (LCPV) technology was developed. Besides the reduction of cost, the LCPV technology also produces clean energy for the building and promotes innovative architectural design. This paper presents a novel type of concentrator for BIPV systems. This concentrator, known as the *rotationally asymmetrical dielectric totally internally reflecting concentrator* (RADTIRC), was incorporated in a small double glazing window. The RADTIRC has a geometrical concentration ratio of 4.9069x. A series of experiments were carried out to evaluate the performance of the solar PV window both indoors and outdoors. It was found that the RADTIRC-PV window increases the short circuit current by 4.13x when compared with a non-concentrating solar PV window. In terms of maximum power generation, the RADTIRC-PV window generates 0.749 W at normal incidence, 4.8x higher than the non-concentrating counterpart.

Keywords: solar photovoltaic; solar concentrator; rotationally asymmetrical concentrator; building integrated photovoltaic system.

1. Introduction

Solar photovoltaic (PV) – a technology that converts solar energy directly into electricity – has great potential in satisfying the world’s energy needs. The 2014 report [1] published by the International Energy Agency (IEA) emphasises that this technology will possibly be the “dominant power source by 2050”. Governments and private sectors have invested a huge amount of money on solar PV technology [2]. In 2014 alone, solar technology attracted approximately USD150 billion¹ (GBP94.5 billion)² worth of investment [2] for funding technology research, development, commercialisation, manufacturing and new projects. To further accelerate the uptake of solar PV, several governments have introduced a number of measures. One of the most effective ones is known as the feed-in tariff (FiT) scheme [3–7]. An FiT scheme pays a consumer a specific tariff per kWh of electricity generated from solar PV technology for a duration of time [8]. The FiT scheme has now been implemented in more than 80 countries [2]. The investment and policies have had a positive effect on solar PV installations worldwide with the cumulative installed capacity of 177 GW by the end of 2014 [2]. From this figure, approximately 49% of these installations were carried out in Europe (see Fig. 1) [2]. It is reported that solar PV was considered as the fastest growing renewable technology in 2014 [2], with an average annual growth rate recorded at 30% when compared with the growth in 2013 [2]. To date, solar PV technology has created approximately 2.5 million jobs around the globe [2].

¹ Here, 1 billion is defined as 1 thousand million, i.e. 10^9 .

² Based on the conversion rate carried out on 10/11/2014, USD1.00 is equivalent to GBP0.63 [34]. This value is used throughout this paper.

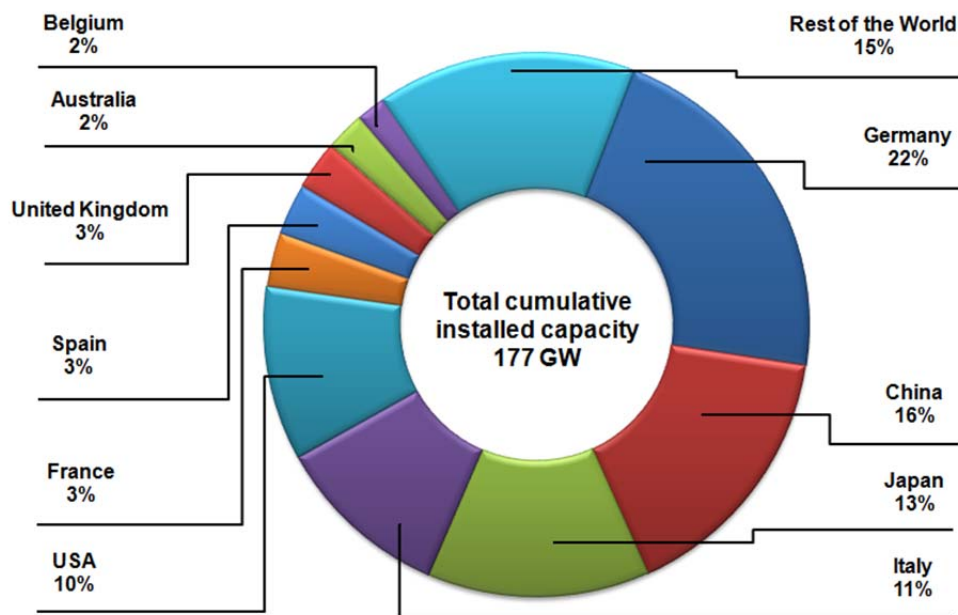


Fig. 1: Cumulative PV installed capacity in 2014. Adapted from [2,9].

Despite the rapid growth in terms of installed capacity, solar PV only supplied around 1% of the world's electricity requirement in 2014 [9]. One of the reasons is the high capital cost of installing a solar PV system, which ranges between USD1200 (GBP756) to USD24000(GBP15120) per kWp according to the recent data from the IEA [10]. The largest proportion of the cost is from the PV module (around 40%) [10], and the PV material contributes up to 73% of the module cost [11], i.e. 29.2% of the overall installation cost. By reducing the usage of PV material in a PV module, it is possible to achieve a cheaper PV system which could further attract more consumers in opting for and installing this technology.

One of the solutions suggested by several researchers to reduce the cost of a solar PV module is to incorporate an optical concentrator into the solar PV design [12]. A concentrator works by focusing the solar energy from a large entrance aperture area to a smaller exit aperture area to which a solar PV cell is attached [12]. By doing this, the amount of PV material can be reduced significantly while maintaining the same electrical output. The concentrator can be fabricated using low cost materials such as plastic or mirrors, which offsets the cost of the displaced PV material [12]. The PV technology that includes a low gain

concentrator (gains $< 10\times$) in the design is known as low-concentration photovoltaics (LCPV).

Researchers have proposed various designs of LCPV in the past 40 years. Pei *et al.* [13] demonstrated that a dielectric Compound Parabolic Concentrator (CPC) extrusion in an LCPV design was capable of increasing the electrical power by 73% when compared with the non-concentrating PV. Another study conducted by Goodman *et al.* [14] showed that a rotationally symmetrical dielectric CPC design increased the short circuit current of the LCPV system by a factor of 5.7x when compared with a bare solar cell. Muhammad-Sukki *et al.* [15] simulated the performance of an extrusion of a dielectric totally internally reflecting concentrator (DTIRC) and concluded that the design could increase the electrical output by nearly 5 times when compared with a non-concentrating system. From their analysis, their LCPV design could reduce the cost by 41% [16]. On the other hand, Sarmah *et al.* [17] showed that an LCPV design employing a dielectric extrusion of asymmetrical CPC produced 2.27 times more electrical power when compared with a system without a concentrator. Their LCPV design could reduce the cost of a solar panel by 20% per kWp [17]. Abu-Bakar *et al.* [18] proposed an LCPV system based on a rotationally asymmetrical CPC which could potentially increase the short circuit current by as much as 6.18 times than the non-concentrating counterpart.

This paper evaluates an LCPV design incorporating a novel concentrator known as the rotationally asymmetrical dielectric totally internally reflecting concentrator (RADTIRC). The authors has recently investigated a new RADTIRC prototype which was created from the polymethyl methacrylate acrylic (PMMA) material by using an injection moulding method and its performance was compared with the old prototype that was created from an acrylic type material known as ‘6091’ by using a silicon moulding technique [19]. The study [19] concluded that the injection moulding technique enables the prototype to achieve a much closer dimension to the desired design than one created from silicon mould, with an area deviation of 0.8%. In terms of the selection of material, the concentrator created from PMMA material provides a much better performance than the ‘6091’ material, an increase of 13.57% in terms of the short circuit current generated at normal incidence [19].

This paper aims to demonstrate that an LCPV system could be created (in this case a small solar PV window) by incorporating an array of 12 concentrators for use in building integration and at the same time could provide substantial electrical output when compared to a similar non-concentrating PV window. The electricity generated can be utilised in the

building, stored in a battery (for off-grid connection) or exported to the grid (for on-grid connection).

2. System description

2.1 Design of optical concentrator

The design of the optical concentrator discussed in this paper, for which there is a patent [20], is discussed in detail in [21]. The creation of the RADTIRC is complex where various 2D templates need to be created at each angle of rotation - with each template has the same total height but has different values of exit aperture width and half-acceptance angle. These two values (i.e. the exit aperture width and the half-acceptance angle) were predetermined by the programme from the input parameters chosen by the users. After 180 of these 2D templates are created, a point cloud is formed by combining all the surface point of these 2D templates to produce the desired RADTIRC. A variety of RADTIRC designs were simulated [21] and one specific design was fabricated and tested indoors and outdoors [22]. The fabricated design has a total height of 3 cm, a square exit aperture of 1 cm by 1 cm, a geometrical concentration ratio³ of 4.9069, an index of refraction of 1.5, two half-acceptance angles which are $\pm 40^\circ$ along the x-axis and $\pm 30^\circ$ along the z-axis (see Fig. 2) [22] to cater for variation of sun path during the day and throughout the year. Although the first prototype yielded a good result, two problems were identified: (i) the dimensions of the concentrator were smaller than the design specifications due to the usage of a silicon mould (see Fig. 3), and (ii) the material used in the prototype suffered a discoloration (from clear to yellowish colour as illustrated in Fig. 3) and photo degradation with time, which reduced its performance by 4% after 2 years. To overcome these problems, the same design was fabricated by UK Optical Plastic Limited using an injection moulding machine BOY 35M [23]. The material chosen for the concentrators is a variation of PMMA resin which is known as Altuglas® V825T and has a refractive index of 1.49 [24]. PMMA is a widely used material for optical concentrators due to its high transmittance (minimum 92%) and good resistance to photo degradation properties [25].

³ For a 3D concentrator, a geometrical concentration ratio is defined as the area ratio of the area of the entrance aperture to the area of the exit aperture [35].

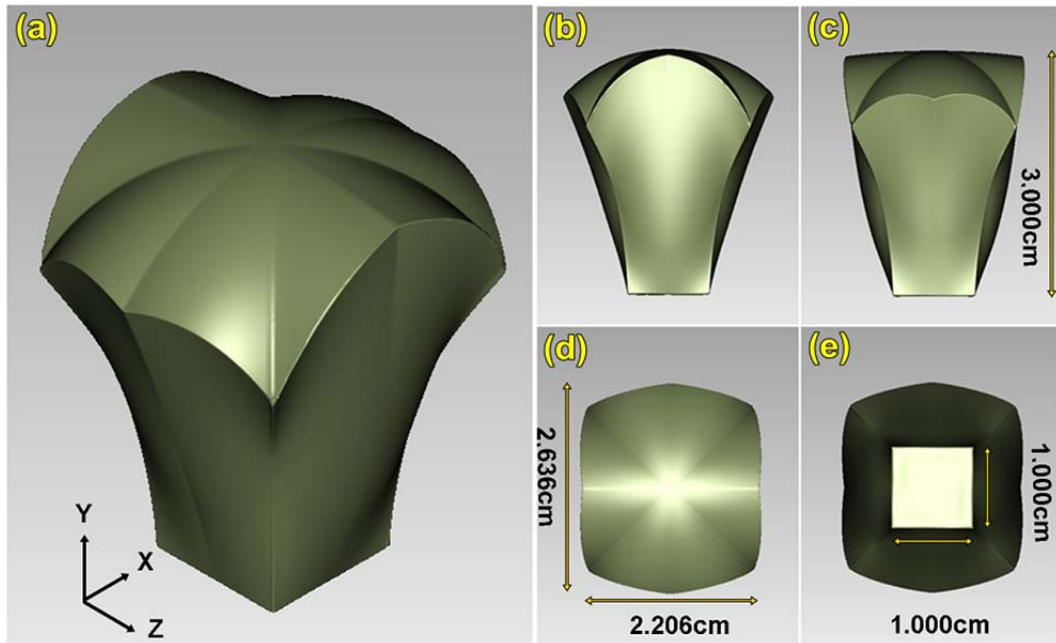


Fig. 2: Prototype RADTIRC dimensions.

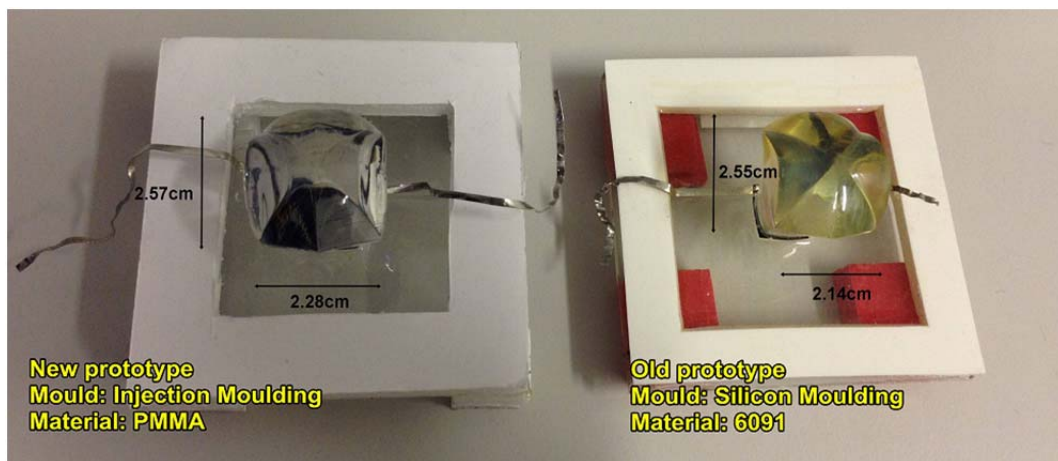


Fig. 3: Comparison of the old and new prototype of the RADTIRC.

2.2 Solar cell

The solar cells used for the test were supplied by Solar Capture Technologies Ltd, United Kingdom and each cell has dimensions of 1 x 1 cm. These monocrystalline silicon solar cells have Laser Grooved Buried Contact (LGBC) and are suitable for LCPV applications [26].

2.3 Assembly process

The small solar PV window prototype⁴ (250mm x 289mm x 70mm) was constructed by utilising 12 RADTIRC prototypes and 12 LGBC cells to create the concentrating-PV windows. The cells were interconnected in series using a pre-design template in a 4 x 3 array (see Fig. 4) and were then glued on a glass substrate. The arrangement of the cells was created in such a way that when the RADTIRCs were placed on the cells, these concentrators achieved the ‘best’ alignment between the cells and the exit aperture of the concentrators to minimise optical losses. The distance between two cell arrays was chosen such that the cells enabled the concentrators to create an optimum and compact arrangement of concentrators. i.e. the concentrators could be placed as close as possible to each other to create the ‘best’ packaging density⁵. The RADTIRC here has a packaging density of 84%.

To permanently mount the concentrators on the solar cells, a silicon elastomer Sylgard-184® from Dow Corning was chosen as the binding material. This material also acts as an encapsulation material for the solar cells and as an index matching gel between the concentrator and the cells [22]. It has a high transmission value of 94.4% [27] and can be cured using a simple process [17,21,25]. The Sylgard-184® was prepared by mixing the supplied base and curing agent in a 10:1 weight ratio in a small beaker. The mixture is then placed in a vacuum chamber for 15 minutes to eliminate air bubbles. A Dow Corning Primer 92-023 was applied on the solar cells for a better adhesion between the Sylgard and the cells. Once the Sylgard was free from air bubbles, the mixture was poured on top of the interconnected cells. Afterwards, the RADTIRCs were placed carefully on top of the solar cells and the elastomer was left to cure for 48 hours under room temperature to ensure good binding between the concentrators and the cells. To compare the performance of this LCPV system with a non-concentrating one, a non-concentrating PV system was created using the same procedure and material.

Both the concentrating and non-concentrating PV systems were sent to Strathclyde Insulating Glass Limited, United Kingdom for assembly within sealed double glazing units

⁴ The length and the width of the window are chosen to fit bricks that are between 215mm and 300mm long according to an EU directive [36].

⁵ Packaging density is defined as the percentage area of the entrance aperture of the concentrator in the entire module area [37]. For example, a square entrance aperture employs a higher packaging density (at 100%) when compared to a circular entrance aperture (at 79%).

and subsequently to Windowplus, United Kingdom to fabricate the window frames. The final form of the solar PV window incorporating the RADTIRC is presented in Fig. 4.



Fig. 4: The solar PV window incorporating the RADTIRC design.

3. Experimental setup

The indoor experimental setup to evaluate the characteristic of the solar window incorporating the RADTIRC is illustrated in Fig. 5. It follows the same setup to evaluate the singular RADTIRC-PV structure which was presented in [19]. A solar simulator (Class AAA, AM 1.5G irradiation spectrum), Oriel® Sol3A Model 94083A, from Newport Corporation was used to simulate direct solar radiation at the earth surface. A variable slope base was placed 38cm beneath the solar simulator's lamp and within the uniform illumination area (20cm x 20cm) of the lamp. A digital tilt meter was used to measure the tilt angle of the variable slope base. A Keithley 2440 source meter with 4-wire connections was utilised here to act as a loading circuit, but with more accuracy [22]. It was connected to a computer which was already installed with Lab Tracer software from National Instruments® to measure the electrical output from both solar windows.

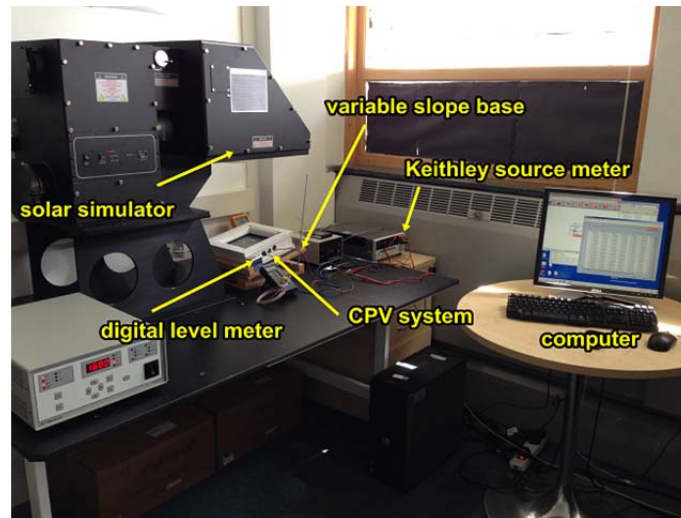


Fig. 5: Indoor experimental setup.

4. Results and discussions

When an array of the RADTIRC-PV cells is connected in series, in theory, the short circuit current generated from the array must be equal to the one generated from a single RADTIRC-PV structure studied previously by the authors in [19]. On the other hand, the maximum power and the open circuit voltage generated by the array will be increased by a factor of 12 since there are 12 RADTIRC-PV cells incorporated in the design. The information from the short circuit current is also needed to compare the opto-electronic gain of the concentrating-PV window with the one produced by the singular RADTIRC-PV structure. However, it is expected some losses will be introduced in the system causing the amount of the short circuit current and the opto-electronic gain produced by the RADTIRC-PV window to be lower than the ones produced by a single RADTIRC-PV structure. The value of the maximum output power (and the open circuit voltage) is also expected to be lower than the theoretically calculated i.e. lower than $12 \times P_{max}$ (and V_{oc}) generated from a single RADTIRC-PV structure.

4.1 The characteristics of the RADTIRC-PV window

The RADTIRC-PV window was placed on the variable slope base. Under the standard test conditions, the solar simulator was configured to produce an irradiance of

1000W/m² and the room temperature was set at 25°C. The door and windows of the room were closed to avoid unwanted air flow and minimise temperature variation and the windows had blinds to prevent light from entering the room. The variable slope was set at 0°. For each measurement, the short circuit current (I_{sc}), the open circuit voltage (V_{oc}), the maximum current (I_{max}), the maximum voltage (V_{max}), the maximum power (P_{max}) and the fill factor (FF) were determined and recorded.

Fig. 6 shows the current-voltage (I-V) characteristics and the power-voltage (P-V) characteristics of the solar PV windows respectively. As it can be seen from Fig. 6, the short circuit current of the non-concentrating window was 0.031 A. However, the introduction of the RADTIRC in the window increased the short circuit current by a factor of 4.13 when compared with the non-concentrating system, generating 0.128 A. As indicated earlier, the concentrator was concentrating the irradiance from the entrance aperture to the exit aperture. This increased the intensity of the light that impinged on the RADTIRC-PV window linearly [28], resulting in a higher short circuit current than the one produced from the non-concentrating window. The open circuit voltage was also increased from 6.65 V to 7.20 V when the RADTIRC-PV window was compared with a non-concentrating PV window. Unlike the short circuit current, the open circuit voltage increased logarithmically with irradiance concentration [28]. The maximum power on the other hand was increased from 0.156 W to 0.749 W when the RADTIRC-PV window was compared with the non-concentrating PV window, giving a maximum power ratio of 4.8. The experiment showed that the RADTIRC-PV window increased the fill factor from 76% to 81% mainly due to an increase in both the short circuit current and the open circuit voltage of the concentrator. In terms of electrical conversion efficiency, the introduction of concentrators in the solar window reduced this value from 13% to 12.72%.

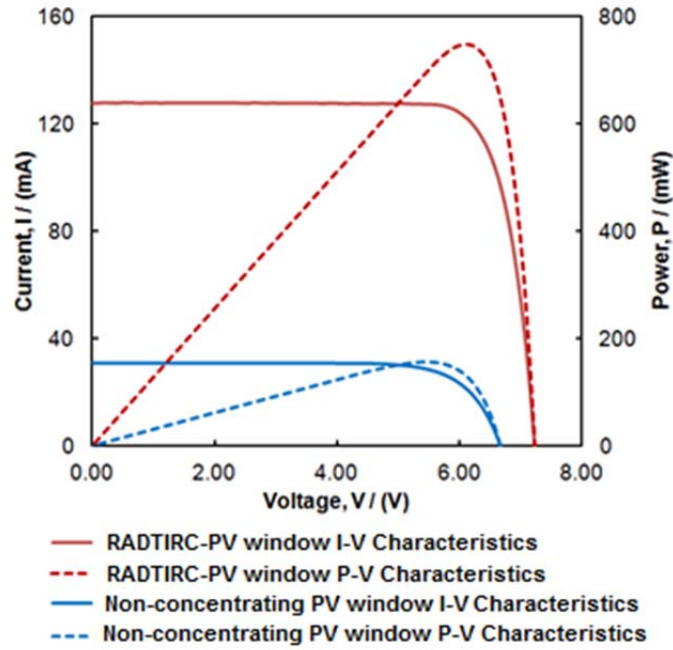


Fig. 6: Electrical outputs from the solar PV windows under standard test conditions.

The output from the RADTIRC-PV window is compared with the result obtained from a single RADTIRC-PV structure studied in [19]. The short circuit current generated from the RADTIRC-PV window decreased to 0.128 A from 0.159 A when compared to the one produced by a single RADTIRC-PV structure, a reduction of 19.4%. The maximum power on the other hand increased by a factor of 9.9 instead of a factor of 12, generating a maximum power value of 75.9 W. As for the non-concentrating PV window, its short circuit current reduced to 0.030 A from 0.036 A when compared to the one produced by a single PV cell, a reduction of 16.7%. In terms of the maximum power generated, the non-concentrating PV window increased this value by 10.1 when compared to amount produced by a single bare cell, achieving a maximum power value of 0.156 W. This losses could be attributed to many factors, including (i) manufacturing errors causing the dimensions of the concentrator to differ from the actual design dimensions, uneven surfaces of the entrance aperture and over polishing on the profile of the side wall; (ii) assembly errors during the soldering of the tabbing wire on the solar cells which reduced the effective area of each cell, misalignment between the solar cells and the exit aperture of the concentrators, misalignment on the arrangement in the arrays of the concentrators along the x and z-axes and losses due to the index matching gel at the lower part of the concentrator profile, and (iii) errors associated

with the rays such as scattering reflection on the front surface of the concentrator which reduces the number of rays reaching the exit aperture of the RADTIRC.

It is also useful to see the variation of I-V and P-V characteristics under various level of solar radiation. The experiment was repeated by varying the output from the solar simulator between 800W/m^2 and 1100W/m^2 and the results are presented in Figs. 7 and 8. When the intensity of the sun simulator increased from 800W/m^2 to 1100W/m^2 , the short circuit current from both solar windows increased - from 0.100A to 0.140A for the RADTIRC-PV window and from 0.025A to 0.034A for the non-concentrating PV window. In terms of the maximum power, the change in simulator's intensities caused the reading from the panels to rise from 0.593W to 0.825W and from 0.125W to 0.170W for the RADTIRC-PV window and the non-concentrating PV window respectively.

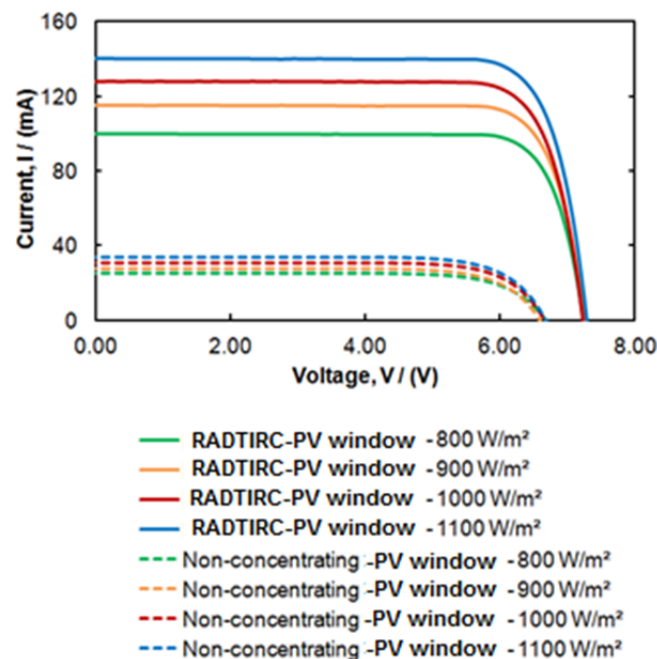


Fig. 7: The I-V characteristics of the solar PV windows under various levels of irradiance.

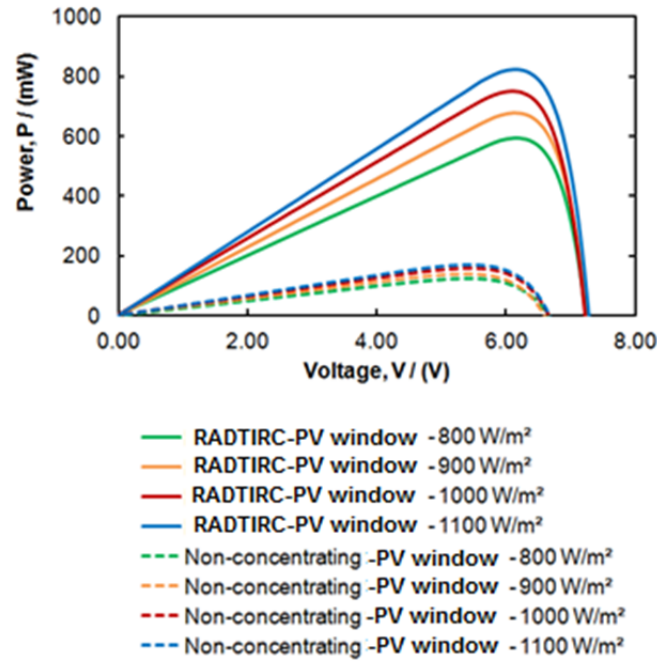


Fig. 8: The P-V characteristics of the solar PV windows under various levels of irradiance.

4.2 The angular response of the RADTIRC-PV window

The next part of the experiment consisted in characterising the angular response of the RADTIRC-PV window. This was carried out by setting the output of the solar simulator at 1000W/m^2 and setting the room temperature at 25°C . The variable slope base was tilted from 0° to 50° at increments of 5° , with each tilt angle measured using the digital level meter. For each angular increment, the short circuit current (I_{sc}), the open circuit voltage (V_{oc}), the maximum current (I_{max}), the maximum voltage (V_{max}), the maximum power (P_{max}) and the fill factor (FF) were determined and recorded.

The variation of the short circuit current is presented in Fig. 9 and the maximum output power of the windows is presented in Fig. 10, both plotted against the incidence angle. In general, both parameters decreased gradually when the angle of incidence increased. From Fig. 9, it was found that the RADTIRC-PV window achieved its maximum short circuit current at normal incidence, with the value of 0.128A recorded. The RADTIRC-PV window achieved 90% of its peak short circuit value when the angle of incidence was at $\pm 15^\circ$ along the x-axis and at $\pm 14^\circ$ along the z-axis. This value reduced to half when the angle of incidence of the rays reached $\pm 25^\circ$. When the angle of incidence was equal to the minimum ‘design’ half-acceptance angle (along the z-axis), the maximum current was always higher

than the one generated from the non-concentrating PV solar window, as illustrated in Fig. 9. Beyond this angle of incidence, the short circuit current continued to decrease eventually reaching a value of 0A.

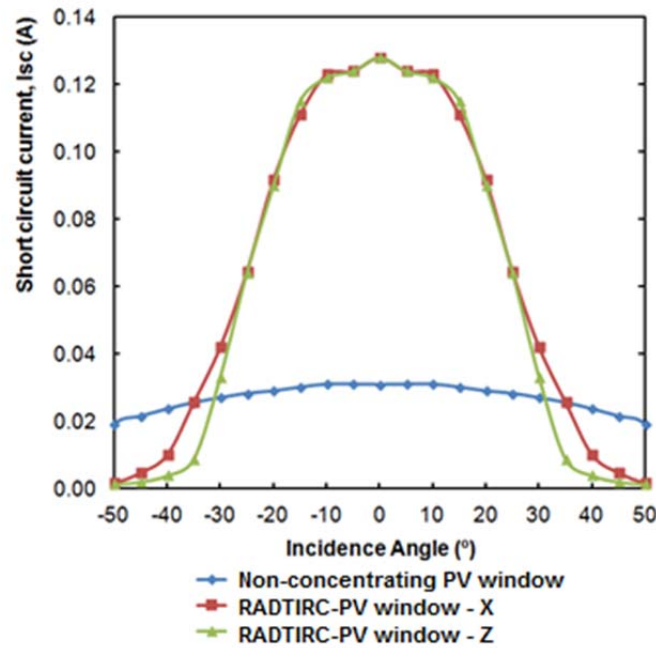


Fig. 9: The short circuit current of the solar PV windows at different angles of incidence.

In terms of maximum output power, the variation of maximum output power against the incidence angle is presented in Fig. 10. When compared with the short circuit current, a similar trend was observed for the values of maximum output power. The peak value of maximum output power was achieved at normal incidence, with the value of 0.749W recorded. The RADTIRC-PV window achieved 90% of its peak short circuit value when the angle of incidence was at $\pm 15^\circ$ along the x-axis and at $\pm 14^\circ$ along the z-axis. This value decreased to half when the angle of incidence of the rays reached $\pm 26^\circ$. When the angle of incidence was equal to the minimum 'design' half-acceptance angle (along the z-axis), the maximum power was always higher than the one produced from the non-concentrating PV window, as indicated in Fig. 10. Beyond this angle of incidence, the maximum power continued to decrease until it reached a value of 0W.

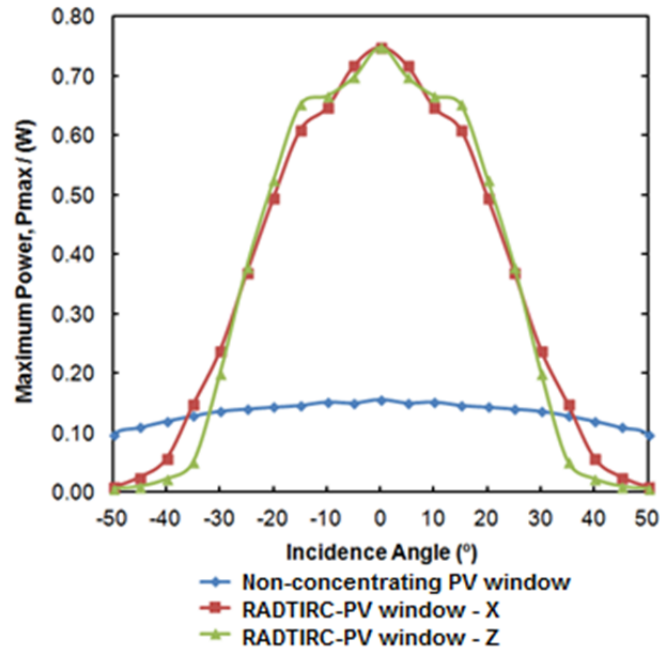


Fig. 10: The maximum power of the solar PV windows at different angles of incidence.

The opto-electronic gain of the concentrator was also plotted against the incidence angle and it is presented in Fig. 11. The opto-electronic gain measures the ratio of short circuit current produced from an LCPV system to the one generated from a conventional non-concentrating one [17,22,29]. The maximum opto-electronic gain was obtained at normal incidence, with a value of 4.13, achieving an optical efficiency of 84%. The RADTIRC-PV window achieved 90% of its peak opto-electronic gain value when the angle of incidence was at $\pm 15^\circ$ along the x-axis and at $\pm 14^\circ$ along the z-axis. This value reduced to half when the angle of incidence of the rays reached $\pm 25^\circ$. When the angle of incidence was equal to the minimum 'design' half-acceptance angle (along the z-axis), the gain was always higher than 1, as indicated in Fig. 11. Outside this incidence angle, the opto-electronic gain dropped gradually to 0.

The opto-electronic gains are compared with the optical gains from the simulations (see Fig. 11). The simulations were carried out using an optical software ZEMAX® and the detail simulation steps have been presented in [21]. The results from the experiment show good agreement with the simulation data, with a deviation of 10% at the peak value. This deviation can be contributed to several factors, which include (i) manufacturing errors causing the dimensions of the concentrator to differ from the actual design dimensions, uneven surfaces of the entrance aperture and over polishing on the profile of the side wall,

and (ii) assembly errors during the soldering of the tabbing wire on the solar cells which reduced the effective area of each cell, misalignment between the solar cells and the exit aperture of the concentrators and misalignment on the arrangement in the arrays of the concentrators along the x and z-axes.

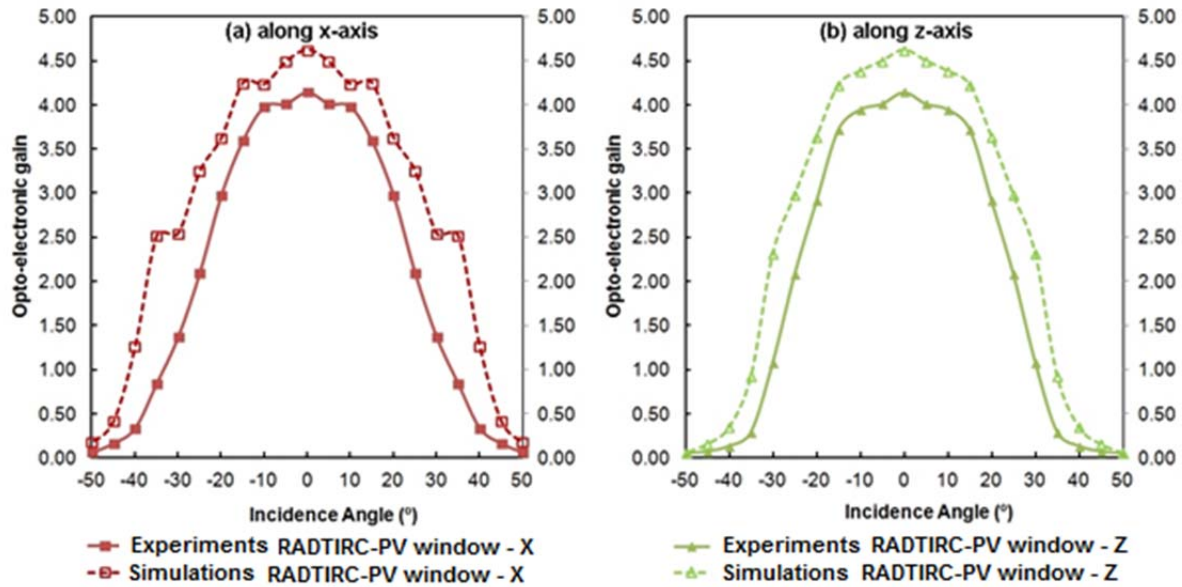


Fig. 11: The optical gain of the RADTIRC-PV window.

The opto-electronic gain generated from the RADTIRC- PV window is also compared to the one produced by a single RADTIRC-PV structure [19], and the results are presented in Figure 12. As expected, the value of the opto-electronic gain of the RADTIRC-PV window is always lower than the one produced by a single RADTIRC-PV structure at all angles of incidence, with a deviation of 7.8% at normal incidence due to losses attributed to several factors described earlier in Section 3.8.1

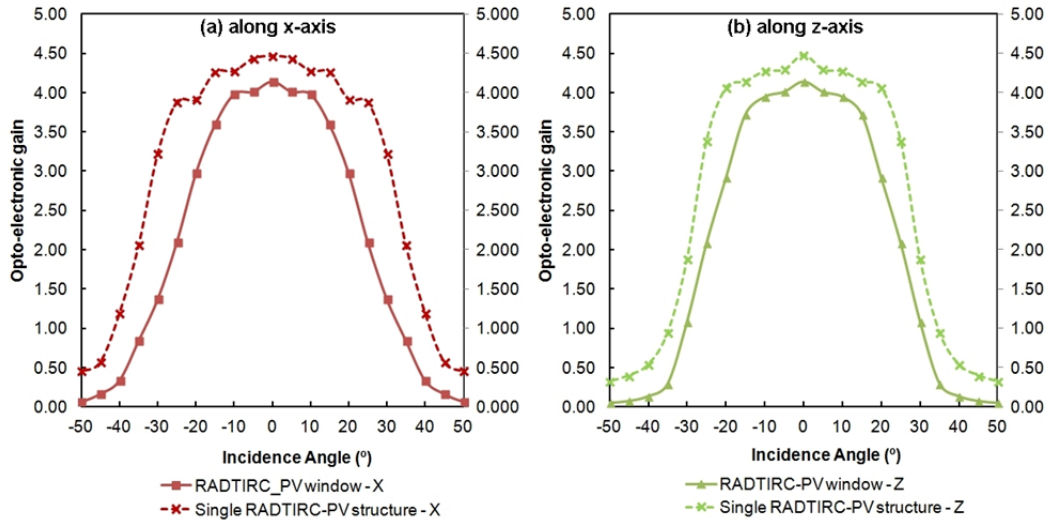


Fig. 12: Comparison of the opto-electronic gain generated from the RADTIRC-PV window and a single RADTIRC-PV structure.

It is also interesting to see that the opto-electronic gain has a large drop when the angle of incidence of the rays was $\pm 20^\circ$ and wider. This was because parts of the RADTIRCs were shaded by the frame of the window (see Figure 13(a)) which reduced the amount of short circuit current from the RADTIRC-PV window. The non-concentrating window experienced the same effect when the angle of incidence of the rays was larger than $\pm 35^\circ$. The largest deviation between the reading of the RADTIRC-PV window and the single RADTIRC-PV structure occurred when the angle of incidence of the rays was at $\pm 30^\circ$ when half of the RADTIRCs were shaded, giving a deviation of 58%. There was no shadowing occurring in the single RADTIRC-PV structure tested in [19] since it was frameless. It is therefore important to ensure that the arrays of the concentrators and the PV cells are integrated in such a way that the shadowing of the cells is avoided in order to maximise the generation of electrical output from the LCPV systems.

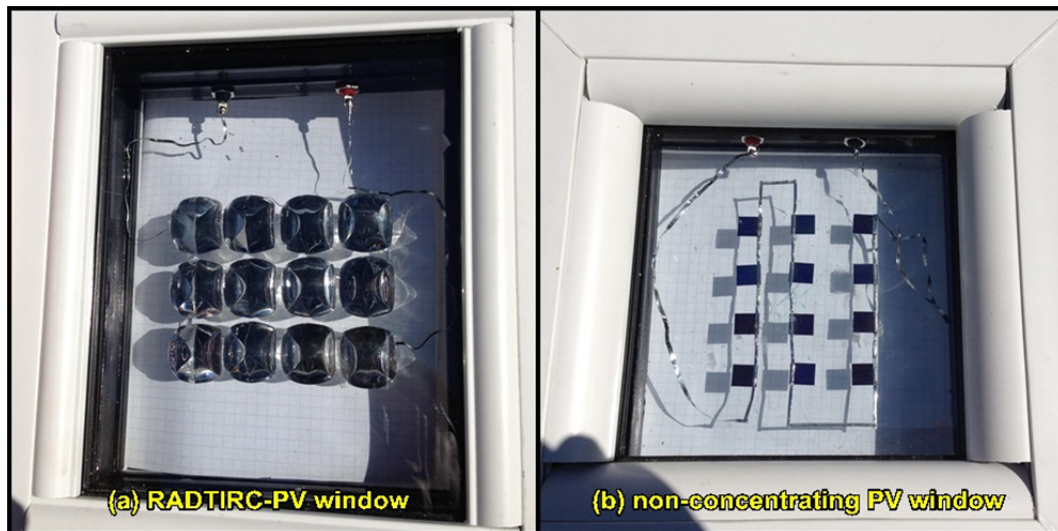


Fig. 13: Shadowing effect on the solar PV windows.

4.3 The effect of temperature on the maximum power generated by the RADTIRC-PV window

This section evaluates the effect of temperature on the performance of the RADTIRC-PV window. For this purpose, two thermocouples were utilised; one was attached at the back of the glass panel beneath one of the solar cells⁶ (see Fig. 14), and another one was used to measure the room temperature. The RADTIRC-PV window was placed at 0° inclination. The solar simulator was configured to produce 1000 W/m² and the room temperature was set at 25°C. The RADTIRC-PV window was exposed to the same radiation for a period of 4.5 hour. A set of readings was taken at intervals of 15 minutes.

⁶ The most accurate way of measuring the temperature would be to place the thermocouple exactly beneath the solar cell. However, based on the heat transfer model using the ANSYS 12.1 software developed by Kumar et al. [38] and Sellami [39] to compare the temperature at the back of the solar cell and at the back of the glass substrate, it was demonstrated that the temperature reading at both location via simulation matched the experimental data accurately. Therefore, this setup is used in this study.

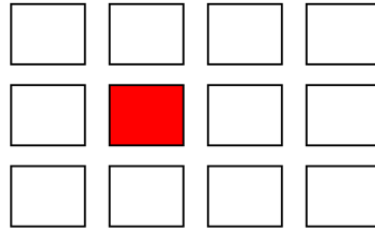


Fig. 14: The top view of the location of the thermocouple (marked in red) attached underneath one of the cells of the RADTIRC-PV window.

Fig. 15 shows the effect of temperature on the maximum power of the RADTIRC-PV window. The temperature of the cell increased sharply from 25°C to 69°C and stabilised after 3 hours. The maximum power reduced from 0.75W to 0.54W, a reduction of 27%. Table 1 presented the variations of the main parameters throughout the duration of the experiment. It was observed that the maximum current showed a slight reduction, from 0.12A to 0.10A. The maximum voltage however showed a considerable fall from 6.12 V to 5.20 V. As for the fill factor, the value reduced from 81% to 79%.

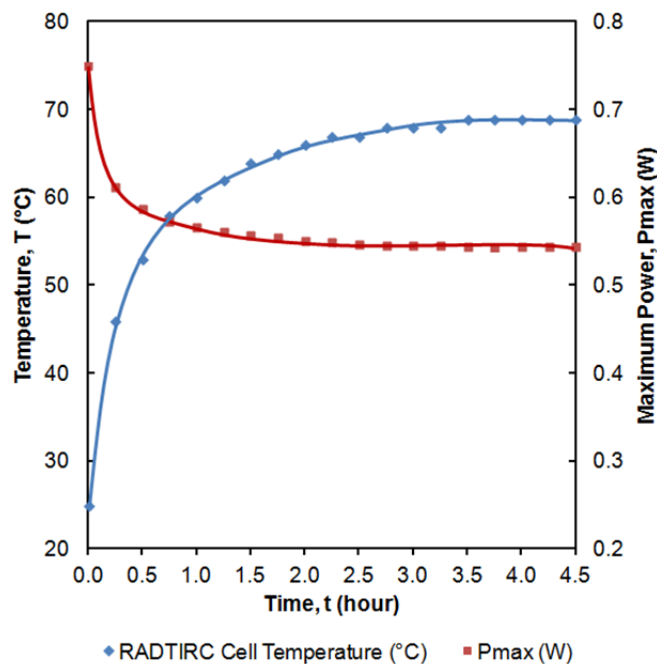


Fig. 15: Variation of RADTIRC-PV cell maximum power and temperature with illumination time.

Table 1: Effect of temperature on the RADTIRC-PV window output.

Time	Room	CPV	V_{\max}	I_{\max}	P_{\max}	V_{oc}	I_{sc}	FF
	Temperatur	Temperatur						
	e	e						
(hour)	(°C)	(°C)	(V)	(A)	(W)	(V)	(A)	
0.00	25	25	6.12	0.12	0.75	7.20	0.13	0.81
0.25	29	46	5.71	0.11	0.61	6.85	0.11	0.80
0.50	30	53	5.51	0.11	0.59	6.65	0.11	0.79
0.75	31	58	5.51	0.10	0.57	6.55	0.11	0.79
1.00	32	60	5.41	0.10	0.57	6.50	0.11	0.78
1.25	32	62	5.31	0.11	0.56	6.45	0.11	0.78
1.50	33	64	5.31	0.10	0.56	6.40	0.11	0.78
1.75	33	65	5.31	0.10	0.55	6.35	0.11	0.79
2.00	33	66	5.20	0.11	0.55	6.35	0.11	0.78
2.25	33	67	5.31	0.10	0.55	6.30	0.11	0.78
2.50	33	67	5.20	0.10	0.55	6.30	0.11	0.78
2.75	33	68	5.20	0.10	0.55	6.30	0.11	0.78
3.00	33	68	5.20	0.10	0.54	6.30	0.11	0.78
3.25	33	68	5.20	0.10	0.54	6.30	0.11	0.78
3.50	33	69	5.20	0.10	0.54	6.25	0.11	0.79
3.75	33	69	5.21	0.10	0.54	6.25	0.11	0.79
4.00	33	69	5.20	0.10	0.54	6.25	0.11	0.79
4.25	33	69	5.20	0.10	0.54	6.25	0.11	0.79
4.50	33	69	5.20	0.10	0.54	6.25	0.11	0.79

414

415

416 It is also useful to identify the temperature coefficient for maximum current,
 417 maximum voltage and maximum power, which are obtained by calculating the ratio of
 418 change in each parameter with respect to the change in temperature [22,30]. It was calculated
 419 that the maximum voltage coefficient was $0.021V/^{\circ}C$, the maximum current coefficient was
 420 $0.454mA/^{\circ}C$ and the maximum power coefficient was $0.005W/^{\circ}C$.

421

5.0 The outdoor experiments

Solar radiation consists of direct and diffuse radiation [31], and each one has a different effect on the performance of the solar PV windows. The outdoor performance of the panels in an open environment has also been investigated. During a sunny day, most of the radiation is direct, but on completely cloudy days, the radiation is mostly diffuse [31]. The outdoor experiments were conducted in Coventry Drive, Glasgow (55.865659°N, 4.21063°W) between 20 June 2014 and 01 July 2014. Both panels were facing true south, (taking into account the magnetic declination of 3.35°W) and were tilted 33° from the horizontal to ensure 0° inclination with respect to the sun elevation angle. The information about the daily sun path and its elevation angle were obtained from [32]. A multimeter was connected to each panel to get simultaneous readings which measure the short circuit current produced by the panels. Simultaneous readings from the multimeters were taken at intervals of 10 minutes for a duration of 10 hours, i.e. from 8.00am until 6.00pm each day.

Fig. 16 shows selected results obtained from the experiment. In general, the introduction of the RADTIRCs increased the short circuit current generated from the panel. Based on the theory and the indoor experiments, the RADTIRC-PV window should produce much higher short circuit current than the non-concentrating system within its 'design' acceptance angle under direct radiation. Based on the sun path information [32], the higher capture time should occur between 11.30am and 2.30pm. This trend can be observed during almost every sunny day (see Fig. 16(a)), where the RADTIRC-PV window generated a much higher short circuit current than the non-concentrated one, which confirms both the theory and the indoor experiments. The maximum short circuit current reading recorded was 114.3mA, much higher than the 30.35mA generated from the non-concentrating PV window. This corresponded to the maximum opto-electronic gain value of 3.77. A similar trend was also observed in a partially sunny day, as illustrated in Fig. 14(b), with the maximum short circuit current generated from the RADTIRC-PV window and non-concentrating PV window being 109.2mA and 28.09mA respectively, providing an opto-electronic gain of 3.89.

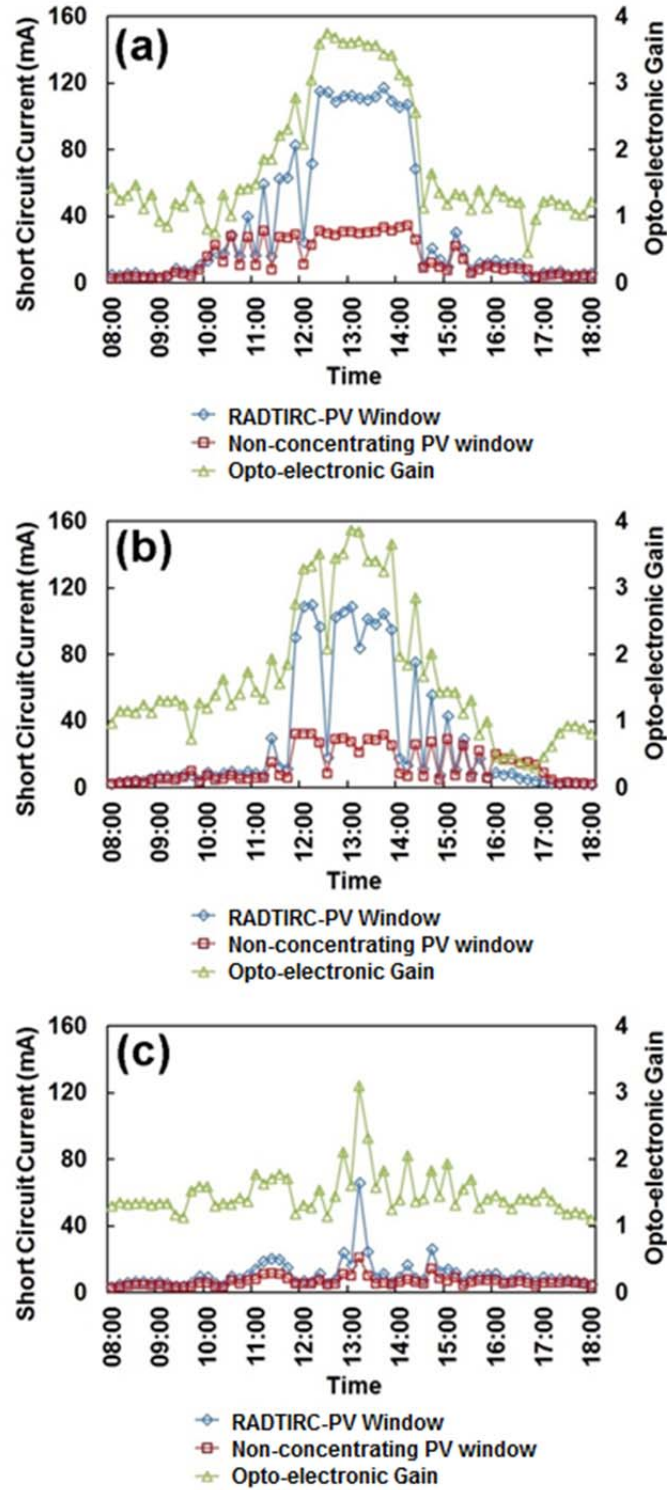


Fig. 16: Results from outdoor experiments; (a) during an almost clear sky day; (b) during a partially clear sky day, and (c) during a cloudy day.

It is interesting to observe the performance of both panels during a cloudy day, and the example is presented in Fig. 14(c). It was observed that the RADTIRC-PV window

performed slightly better than the non-concentrating counterpart throughout the cloudy day, giving an opto-electronic gain value of minimum 1.1 for the whole period of 10 hours. This indicates that outside the 'design' half-acceptance angles of the concentrator, the diffuse radiation is still collected from the entrance aperture as well as the side profile of the concentrator to reach the solar cells, hence increasing the short circuit current generated from the solar windows.

From the observations during sunny and cloudy days, it is possible to conclude that the RADTIRC is capable to increase the short circuit current generated from the window. It is argued that the panel could not achieve its peak opto-electronic gain due to some factors. These include misalignment of the panels with reference to the sun path, errors in positioning the panel to face the true south, the frequently varying solar insolation, the formation of clouds, as well as changes in wind speed which caused the gain to reduce significantly.

Conclusions

A new type of solar window incorporating a novel RADTIRC design was proposed for BIPV system. The steps to assemble a RADTIRC-PV cells array within a double glazed window have been explained in detail. This panel underwent a series of analysis both indoors and outdoors and these results were compared with a non-concentrating panel. From the indoor experiments, it was found that the introduction of the RADTIRCs in the window could increase the short circuit current by a factor of 4.13 when compared with the non-concentrating PV system, generating 0.128 A. The maximum power on the other hand was increased from 0.156 W to 0.749 W when the RADTIRC-PV window was compared with the non-concentrating PV window, giving a maximum power ratio of 4.8. The output from the RADTIRC-PV window was also compared with the result obtained from a single RADTIRC-PV structure studied previously by the author in [19]. The short circuit current generated from the RADTIRC-PV window decreased to 0.128 A from 0.159 A when compared to the one produced by a single RADTIRC-PV structure, a reduction of 19.4%. The maximum power on the other hand increased by a factor of 9.9 instead of a factor of 12, generating a maximum power value of 75.9. As for the non-concentrating PV window, its short circuit current reduced to 0.030 A from 0.036 A when compared to the one produced by a single PV cell, a reduction of 16.7%. In terms of the maximum power generated, the non-concentrating PV window increased this value by 10.1 when compared to the amount produced by a single bare cell, achieving a maximum power value of 0.156 W. These losses could be attributed to

many factors, including manufacturing errors, assembly errors and errors associated with the rays which reduce the number of rays reaching the exit aperture of the RADTIRC.

In terms of the opto-electronic gain, it was also found that within the minimum 'design' half-acceptance angle of the RADTIRC, the opto-electronic gain of the RADTIRC-PV window was always higher than 1, with a maximum value of 4.13x. The opto-electronic gain was also compared with the simulation and the results from the experiment showed good agreement with the ZEMAX® simulations. The opto-electronic gain generated from the RADTIRC- PV window was also compared to the one produced by a single RADTIRC-PV structure. As expected, the value of the opto-electronic gain of the RADTIRC-PV window was always lower than the one produced by a single RADTIRC-PV structure at all angles of incidence, with a deviation of 7.8% at normal incidence due to losses attributed to several factors described earlier in the previous paragraph, as well as due to shading from the frame of the windows. In terms of effect of the temperature on the performance of the RADTIRC-PV window, it was demonstrated that the maximum steady state temperature of the panel for the experimental setup used was 69°C, achieved within 3 hours of exposure to the sun. The corresponding maximum power during the steady state was recorded at 0.54W. The maximum voltage coefficient, the maximum current coefficient and the maximum power coefficient were determined to be 0.021V/°C, 0.454mA/°C and 0.005W/°C. As for the outdoor experiments, the variations of short circuit current and opto-electronic gain were plotted for a duration of 10 hours for several days. Under direct radiation, the RADTIRC-PV window generated a maximum opto-electronic gain of 3.89 while under diffuse radiation, the opto-electronic gain varied with a minimum value of 1.1.

It can be concluded that the RADTIRC has the potential to increase the electrical output from a solar window. Within the half-acceptance angle of the RADTIRC, the short circuit current and the maximum power are always higher than the ones generated from non-concentrating PV window. Despite this advantage, a longer exposure to the sun could increase the temperature of the cells in the window, which will reduce the maximum power of the RADTIRC-PV window - in this paper by 27%. It is therefore desirable to reduce the temperature of the cells to ensure a maximum output from the RADTIRC-PV window. This can be achieved by introducing a hybrid/thermal system using air that utilises the co-generated heat to stimulate ventilation in the building [15,21,33].

This paper demonstrated that an LCPV structure (in this case a solar PV window) could be constructed for use in a BIPV system. The LCPV design could also provides substantial gain in the electrical output when compared to a non-concentrating PV design. However, careful consideration is required to minimise the losses in the system.

Some of the future work that could be investigated include (i) detailed analysis on the effect of diffuse radiation on the windows' performance; (ii) long term evaluation of the windows outdoors, (iii) prediction of electrical output for a particular location based on meteorological data, and (iv) analysis of PV window incorporating a different variation of RADTIRC which could produce more energy specifically for vertical integration in a building.

Acknowledgments

This project is funded by Glasgow Caledonian University (GCU), Scotland's Energy Technology Partnership (ETP) and Majlis Amanah Rakyat (MARA), Malaysia. The authors would like to acknowledge the collaboration of AES Ltd. and its contribution to this project. Thanks are due to Mr Ian Baistow from Solar Capture Technologies Ltd, United Kingdom for providing the solar cells, Mr Antoine Y Messiou from UK Optical Plastics Limited, United Kingdom for fabricating the concentrators, Mr Mark Kragh from Off- Grid Europe, Germany for supplying the tabbing wire, Mr Martin Blore from Strathclyde Insulating Glass Limited, United Kingdom for creating the sealed double glazing unit, Mr Robert Tierney from Windowplus, United Kingdom for fabricating the window frame and Mr Robert Adamson from Glasgow Caledonian University, United Kingdom for creating the connections in the solar window panels.

References

- [1] IEA. Energy Technology Perspectives 2014: Executive Summary. 2014.
- [2] REN21. Renewables 2015 Global Status Report. France: 2015.
- [3] Ahmad S, Tahar RM, Muhammad-Sukki F, Munir AB, Rahim RA. Role of feed-in tariff policy in promoting solar photovoltaic investments in Malaysia: A system dynamics approach. Energy 2015;84:808–15.

- 554 [4] Gallego-Castillo C, Victoria M. Cost-free feed-in tariffs for renewable energy deployment in
555 Spain. *Renewable Energy* 2015;81:411–20.
- 556 [5] Huenteler J. International support for feed-in tariffs in developing countries—A review and
557 analysis of proposed mechanisms. *Renewable and Sustainable Energy Reviews* 2014;39:857–
558 73.
- 559 [6] Tsai W-T. Feed-in tariff promotion and innovative measures for renewable electricity: Taiwan
560 case analysis. *Renewable and Sustainable Energy Reviews* 2014;40:1126–32.
- 561 [7] Campoccia A, Dusonchet L, Telaretti E, Zizzo G. An analysis of feed-in tariffs for solar PV in
562 six representative countries of the European Union. *Solar Energy* 2014;107:530–42.
- 563 [8] Muhammad-Sukki F, Munir AB, Ramirez-Iniguez R, Abu-Bakar SH, Mohd Yasin SH,
564 McMeekin SG, et al. Solar photovoltaic in Malaysia: The way forward. *Renewable and*
565 *Sustainable Energy Reviews* 2012;16:5232–44.
- 566 [9] IEA-PVPS. 2014 Snapshot of Global PV Markets. 2015.
- 567 [10] IEA-PVPS. Trends 2015 in Photovoltaic Applications. 2015.
- 568 [11] Goodrich A, Hacke P, Wang Q, Sopori B, Margolis R, James TL, et al. A wafer-based
569 monocrystalline silicon photovoltaics road map: Utilizing known technology improvement
570 opportunities for further reductions in manufacturing costs. *Solar Energy Materials and Solar*
571 *Cells* 2013;114:110–35.
- 572 [12] Muhammad-Sukki F, Ramirez-iniguez R, Mcmeekin SG, Stewart BG, Clive B. Solar
573 Concentrators. *International Journal of Applied Sciences* 2010;1:1–15.
- 574 [13] Pei G, Li G, Su Y, Ji J, Riffat S, Zheng H. Preliminary Ray Tracing and Experimental Study
575 on the Effect of Mirror Coating on the Optical Efficiency of a Solid Dielectric Compound
576 Parabolic Concentrator. *Energies* 2012;5:3627–39.
- 577 [14] Goodman NB, Ignatius R, Wharton L, Winston R. Solid-dielectric compound parabolic
578 concentrators: on their use with photovoltaic devices. *Applied Optics* 1976;15:2434–6.
- 579 [15] Muhammad-Sukki F, Ramirez-Iniguez R, McMeekin S, Stewart B, Clive B. Optimised
580 Dielectric Totally Internally Reflecting Concentrator for the Solar Photonic Optoelectronic
581 Transformer System: Maximum Concentration Method. In: Setchi R, Jordanov I, Howlett R,
582 Jain L, editors. *Knowledge-Based and Intelligent Information and Engineering Systems SE -*
583 *67*, vol. 6279, Springer Berlin Heidelberg; 2010, p. 633–41.
- 584 [16] Muhammad-Sukki F, Ramirez-Iniguez R, McMeekin SG, Stewart BG, Clive B. Optimisation
585 of Concentrator in the Solar Photonic Optoelectronic Transformer : Comparison of
586 Geometrical Performance and Cost of Implementation. *International Conference on*
587 *Renewable Energies and Power Quality (ICREPQ'11)*, Las Palmas de Gran Canaria, Spain:
588 2011, p. 1–6.
- 589 [17] Sarmah N, Richards BS, Mallick TK. Design, development and indoor performance analysis
590 of a low concentrating dielectric photovoltaic module. *Solar Energy* 2014;103:390–401.

- 591 [18] Abu-Bakar SH, Muhammad-Sukki F, Ramirez-Iniguez R, Mallick TK, Munir AB, Mohd
592 Yasin SH, et al. Rotationally asymmetrical compound parabolic concentrator for concentrating
593 photovoltaic applications. *Applied Energy* 2014;136:363–72.
- 594 [19] Abu-Bakar SH, Muhammad-Sukki F, Freier D, Ramirez-Iniguez R, Mallick TK, Munir AB, et
595 al. Optimisation of the performance of a novel rotationally asymmetrical optical concentrator
596 design for building integrated photovoltaic system. *Energy* 2015;90:1033–45.
- 597 [20] Ramirez-iniguez R, Muhammad-Sukki F, McMeekin SG, Stewart BG. Optical element. Patent
598 No. 2497942, 2014.
- 599 [21] Muhammad-Sukki F, Abu-bakar SH, Ramirez-iniguez R, McMeekin SG, Stewart BG, Sarmah
600 N, et al. Mirror symmetrical dielectric totally internally reflecting concentrator for building
601 integrated photovoltaic systems. *Applied Energy* 2014;113:32–40.
- 602 [22] Muhammad-Sukki F, Abu-Bakar SH, Ramirez-Iniguez R, McMeekin SG, Stewart BG, Munir
603 AB, et al. Performance analysis of a mirror symmetrical dielectric totally internally reflecting
604 concentrator for building integrated photovoltaic systems. *Applied Energy* 2013;111:288–99.
- 605 [23] Messiou A. Y. UK Optical Plastics Ltd. Available from
606 [Http://www.ukopticalplastics.com/index.html](http://www.ukopticalplastics.com/index.html) Last Accessed on 10 November 2014.
- 607 [24] ARKEMA GROUP. Standard range - Altuglas® acrylic resins. Available from
608 [Http://www.altuglas.com/en/resins/resins-by-Performance/standard-Range/index.html](http://www.altuglas.com/en/resins/resins-by-Performance/standard-Range/index.html) - Last
609 Accessed on 10 Nov 2014.
- 610 [25] Sarmah N. Design and Performance Evaluation of a Low Concentrating Line-axis Dielectric
611 Photovoltaic System. PhD Thesis, Heriot-Watt University, United Kingdom, 2012.
- 612 [26] Solar Capture Technologies. Cells. Available from
613 [Http://solarcapturetechnologies.com/services/manufacturing/cells](http://solarcapturetechnologies.com/services/manufacturing/cells) Last Accessed on 10 Nov
614 2014.
- 615 [27] Kempe MD. Accelerated UV test methods and selection criteria for encapsulants of
616 photovoltaic modules. 2008 33rd IEEE Photovoltaic Specialists Conference, IEEE; 2008, p. 1–
617 6.
- 618 [28] Volker Quaschnig. *Understanding Renewable Energy Systems*. Earthscan; 2004.
- 619 [29] Ning X, Winston R, O’Gallagher J. Dielectric totally internally reflecting concentrators.
620 *Applied Optics* 1987;26:300–5.
- 621 [30] Mammo ED, Sellami N, Mallick TK. Performance analysis of a reflective 3D crossed
622 compound parabolic concentrating photovoltaic system for building façade integration.
623 *Progress in Photovoltaics: Research and Applications* 2013;21:1095–103.
- 624 [31] Hankins M. *Stand-alone Solar Electric Systems: The Earthscan Expert Handbook for
625 Planning, Design and Installation*. Earthscan; 2010.
- 626 [32] University of Oregon USA. Sun path chart program. Availabe from
627 <http://solardat.uoregon.edu/SunChartProgram.html> Last Accessed on 10 June 2014.

- 628 [33] Kumar R, Rosen MA. A critical review of photovoltaic–thermal solar collectors for air
629 heating. *Applied Energy* 2011;88:3603–14.
- 630 [34] X-Rates. 2014. Currency Calculator. Available from <http://www.x-rates.com/calculator/>. Last
631 accessed on 10 March 2014.
- 632 [35] Welford WT, Winston R. *High Collection Nonimaging Optics*. Academic Press; 1989.
- 633 [36] MojoCorp Ltd. 2015. Common window sizes. Available from
634 <http://www.simplifydiy.com/windows-and-doors/windows/window-sizes>. Last accessed on 20
635 December 2015.
- 636 [37] Solanki CS. *Solar Photovoltaics: Fundamentals, Technologies And Applications*. 3rd ed. PHI
637 Learning; 2015.
- 638 [38] Sendhil Kumar N, Matty K, Rita E, Simon W, Ortrun A, Alex C, et al. Experimental validation
639 of a heat transfer model for concentrating photovoltaic system. *Applied Thermal Engineering*
640 2012;33-34:175–82.
- 641 [39] Sellami N. *Design and characterisation of a novel translucent solar concentrator*. PhD Thesis,
642 Heriot-Watt University, United Kingdom, 2013.
- 643